

## Article

# A Green Nanocatalyst for Fatty Acid Methyl Ester Conversion from Waste Cooking Oil

Sadaf Khosa <sup>1</sup>, Madeeha Rani <sup>1</sup>, Muhammad Saeed <sup>2</sup>, Syed Danish Ali <sup>3</sup>, Aiyeshah Alhodaib <sup>4,\*</sup>  and Amir Waseem <sup>1,\*</sup> 

<sup>1</sup> Department of Chemistry, Quaid-i-Azam University, Islamabad 45320, Pakistan

<sup>2</sup> School of Chemistry, University of the Punjab, Lahore 54590, Pakistan

<sup>3</sup> Nanoscience and Technology Department, National Centre for Physics, Islamabad 44000, Pakistan

<sup>4</sup> Department of Physics, College of Science, Qassim University, Buraydah 51452, Saudi Arabia

\* Correspondence: ahdieb@qu.edu.sa (A.A.); amir@qau.edu.pk (A.W.)

**Abstract:** This study used a novel combination of cellulose nanocrystals (CNCs) and calcium oxide (CaO) nanocomposite (CaO/CNCs) for the production of biodiesel from waste cooking oil. The filter paper was used as a raw cellulose source to produce the CNCs from the acid hydrolysis of cellulose with sulfuric acid. The as-synthesized CaO/CNC nanocomposite is recyclable and environmentally friendly and was characterized using Fourier transform infrared spectroscopy, energy dispersive X-ray, scanning electron microscopy, and X-ray diffraction. The optimum process parameters investigated are a 20:1 methanol-to-oil molar ratio, 3-weight percent catalyst concentration, 60 °C temperature, and 90 min of reaction time. Under the optimum conditions, a biodiesel yield of 84% was obtained. The CaO/CNC nanocomposite achieved five times reusability, indicating its effectiveness and reusability in the transesterification reaction. The synthesized biodiesel chemical composition was examined using FTIR, GCMS, <sup>1</sup>H-NMR, and <sup>13</sup>C-NMR, and its properties, including specific gravity, color, flash point, cloud point, pour point, viscosity, sulfur content, sediments, water content, total acid number, cetane number, and corrosion test, were ascertained using ASTM standard practices. The outcomes were determined to fulfill global biodiesel standards (ASTM 951, 6751). Five successive transesterification processes were used to test the regeneration of the catalyst; the first three showed no distinct change, while the fifth cycle showed a reduction of up to 79%. The innovative composite CaO/CNC and used cooking oil are stable, affordable, and extremely successful for long-term biodiesel generation.

**Keywords:** biofuel; cellulose nanocrystals; CaO nanoparticles; environmental sustainability; transesterification; waste cooking oil



**Citation:** Khosa, S.; Rani, M.; Saeed, M.; Ali, S.D.; Alhodaib, A.; Waseem, A. A Green Nanocatalyst for Fatty Acid Methyl Ester Conversion from Waste Cooking Oil. *Catalysts* **2024**, *14*, 244. <https://doi.org/10.3390/catal14040244>

Academic Editors: José María Encinar Martín and Sergio Nogales Delgado

Received: 18 March 2024

Revised: 4 April 2024

Accepted: 4 April 2024

Published: 6 April 2024



**Copyright:** © 2024 by the authors. Licensee MDPI, Basel, Switzerland. This article is an open access article distributed under the terms and conditions of the Creative Commons Attribution (CC BY) license (<https://creativecommons.org/licenses/by/4.0/>).

## 1. Introduction

Generally, renewable energy serves an important role in dealing with climate change and energy security challenges at the local, national, and worldwide levels. Most prosperous countries have made substantial strides toward reducing their reliance on fossil fuels through the excessive use of alternate and renewable energy sources. Despite these tremendous efforts, there is still an intense preference for energy derived from fossil fuels. However, despite the rapid development of technology, the transportation sector has consistently seen an increase in demand for oil [1]. Fossil fuels comprise 85% of the world's energy sources in today's world and are predicted to remain so throughout the foreseeable future as well [1]. It was pointed out that climate change has the greatest effect on the production of biomass, being a renewable energy source [2]. To solve these issues, suitable replacements for environmentally friendly fuels must be developed and put into practice. To replace fossil fuels like oil, coal, and diesel oil, appropriate, clean, and renewable energy sources have been the subject of much research, both in the past and present [2,3].

Fatty acid methyl esters (FAMEs), another name for biodiesel, are typically made by catalytically transesterifying vegetable or animal fats with methanol. Esterification and transesterification are the primary processes used in the manufacturing of biodiesel [4]. Researchers have centered on problems including (1) inexpensive raw materials, (2) reusable catalysts, and (3) effective reactors to carry out transesterification reactions to accomplish sustainable goals in the production of biodiesel [5–7]. In addition to that, the conversion of biomass to biofuels and life cycle assessment is also one of the most important aspects for policy decisions as biofuels should be based on evidence that biofuels are produced in a sustainable manner [8]. Thus, to produce biodiesel, it must be feasible to recognize widely accessible and unused feedstocks. Animal fats, used cooking oil, and non-edible seed oils have all expanded their availability as both environmentally and economically acceptable feedstocks for the generation of biofuels in recent years [3,9–12]. Among the many energy sources, biodiesel is biodegradable, sustainable, and non-toxic [5,13,14]. Both edible and nonedible vegetable oils as well as animal fats are possible sources of biodiesel feedstock. Yet, edible oils are not favored for the synthesis of biodiesel because of their high price, limited stock, and probable general consequences [15]. The general cost of manufacturing has decreased as a result of the widespread use of waste cooking oil (WCO) as a feedstock for biodiesel production. Moreover, using WCO as a feedstock can aid in addressing issues with environmental degradation [16].

Calcium oxide (CaO) is inexpensive and is one of several potential catalytic compositions; however, it is very relevant because of its high basicity, low toxicity, accessibility, and affordability. Numerous studies have shown that CaO alone leaves calcium ions in methanol if left in contact for a long time; therefore, CaO composite formation is recommended to avoid the use of decalcifying agents at an additional cost to ensure high purity in the end products [17,18]. However, the use of pristine CaO is limited by its long reaction time, and much interest has been shown in modifying pristine CaO to enhance reaction rates and basic active sites [19–21]. The emergence of cellulose nanocrystals (CNCs) as a novel class of nanomaterials can be attributed to their renewable, environmentally harmless, naturally occurring, biodegradable, and biocompatible properties [22]. Furthermore, CNCs have a large number of hydroxyl groups on their surface; and the surface sulfate ester groups in CNCs are produced by hydrolysis with sulfuric acid, which helps to stabilize metal nanoparticles (mNPs). Because of their exceptional qualities, researchers have focused a lot of attention on the use of CNCs in the production of mNP catalysts, which act as excellent support for heterogeneous catalysts [23]. Using waste material as a source for catalyst synthesis with active metal modification can thus be viewed as a viable strategy for producing cost-effective product biodiesel. For example, one study reported composites of CaO utilizing solid coconut waste as oil and eggshells as a CaO catalyst supported with polyvinyl alcohol (PVA) in a packed bed reactor. The biodiesel yield of 95% was obtained at a reaction temperature of 61 °C and reaction time of 3 h with a catalyst loading (CaO/PVA) of 2.29 wt.% [21]. In a similar study, a PVA-supported CaO/CNC/PVA catalyst was synthesized and utilized for biodiesel production from WCO in a packed bed reactor. Chicken bone and coconut residue were used as sources for CaO and CNC, and the supported catalyst (0.5 wt.%) was able to yield 98.40% biodiesel at 65 °C with a sufficiently large reaction time of 4 h [24]. Similarly, CaO (calcined from eggshells) supported on silica, which is obtained from treated waste glassware and further modified by impregnating cerium oxide to increase activity, acts as a bifunctional catalyst for the conversion of beef fat to biodiesel [20].

In this research, a calcium oxide and cellulose nanocrystal (CaO/CNC) nanocomposite was synthesized through the hydrothermal method without using support material. The cellulose source used was filter paper as a reference for CNC (cellulose nanocrystal) synthesis through acid hydrolysis; however, it can be replaced in the future by sustainable cellulose sources coming from wastes or residual biomass. The CaO/CNC nanocomposite, being a heterogeneous catalyst, offers a lack of sensitivity to free fatty acids, is non-corrosive in nature, and can be regenerated, reused, and separated easily from the product. Common

laboratory filter paper, which is commercially available as a source of CNCs, is combined with CaO nanoparticles and employed as catalysts to assess their catalytic performance in the transesterification process for biodiesel production. The CaO/CNC catalyst underwent thorough characterization via techniques, i.e., SEM, EDX, XRD, and FTIR. The nanocomposite was utilized to produce biodiesel from waste cooking oil.

## 2. Results and Discussion

### 2.1. Catalyst Characterizations

#### 2.1.1. X-ray Diffraction

The X-ray diffraction patterns of CaO, CNC, and CaO/CNC composites were examined. In close agreement with reference card no JCPDS 00-02-1088 (Joint Committee on Powder Diffraction Standards) using the software X'Pert HighScore<sup>®</sup>, version 2.1.1, the XRD pattern of CaO revealed distinctive peaks at  $2\theta$  values of  $32.34^\circ$ ,  $37^\circ$ ,  $54.23^\circ$ , and  $63.47^\circ$ , which, respectively, correspond to lattice planes (111), (200), (220), and (311) (Figure 1a,d).

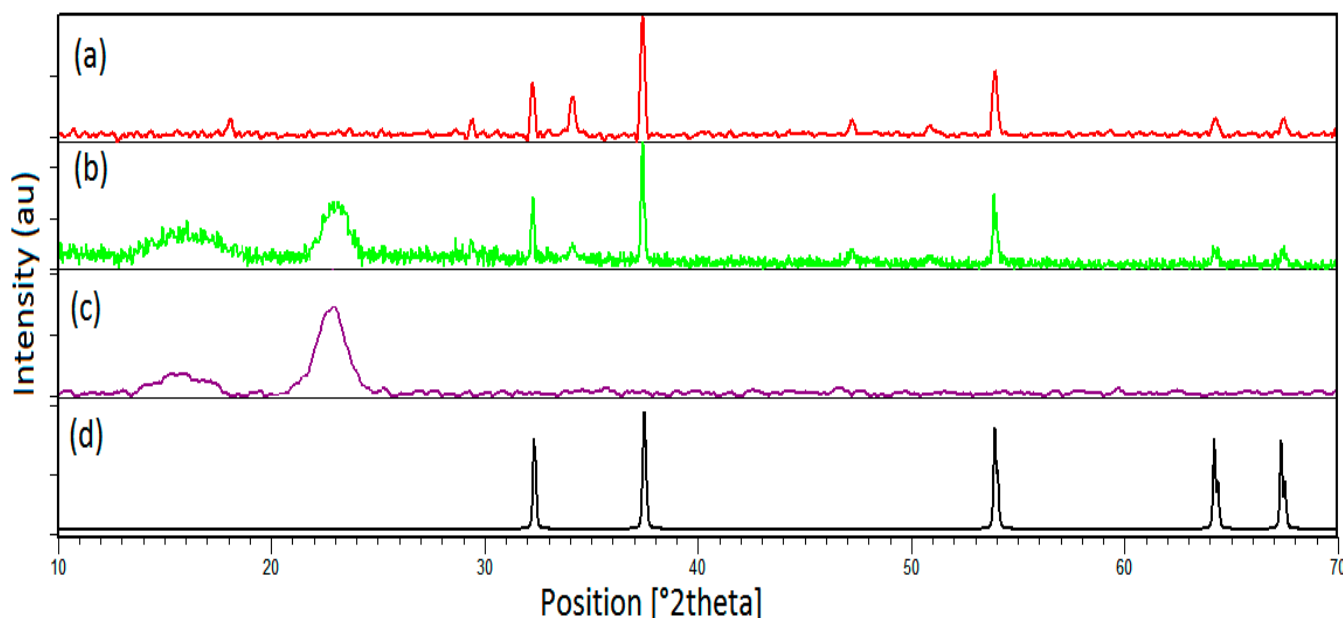


**Figure 1.** XRD patterns of (a) CaO, (b) CNC/CaO, and (c) CNC and (d) the standard reference pattern of CaO (JCPDS 00-02-1088).

In the case of CNCs, the XRD examination revealed two broad diffraction peaks at 15.1–17.5 and 22.7, which, as previously reported [25], correspond to the crystal planes (101), (101), and (002) of cellulose type I. (Figure 1c). Similar peaks to those of CaO and CNC were visible in the CaO/CNC composite; however, some peak intensities decreased as the composite formed (Figure 1b). The XRD pattern corroborated the calculated average crystalline size of 42 nm, which indicates the successful synthesis of the composite.

#### 2.1.2. FTIR

The vibrational bands contained in CaO nanoparticles, CNC, and the CaO/CNC composite in the region of  $4000\text{--}400\text{ cm}^{-1}$  were examined using the FTIR technique (Figure 2). The peak in the range of  $500\text{--}450\text{ cm}^{-1}$ , due to the M–O bond present in CaO nanoparticles, as reported earlier, and the peak at  $874$  and  $1418\text{ cm}^{-1}$  corresponding to the C–O bond, suggesting the carbonation of calcium oxide, were both seen in the spectra of CaO [26,27]. Peaks in CNC include the following: –OH stretch ( $3600\text{--}3200\text{ cm}^{-1}$ ), C–H stretch of cellulose polysaccharides ( $2910\text{ cm}^{-1}$ ), –OH bending vibration ( $1640\text{ cm}^{-1}$ ),  $\text{CH}_2$  bending ( $1430\text{ cm}^{-1}$ ), and  $1372\text{ cm}^{-1}$  ( $\text{CH}_3$  bending), and –CO stretching ( $1060$ ). Each of the positive detected peaks is in conformity with the published literature [28]. The peaks at  $874$  and

1418  $\text{cm}^{-1}$  in the composite CaO/CNC FTIR spectrum are caused by CaO nanoparticles, which are not present in the CNC spectra. The peak of calcium oxide's carbonation coincided with the  $\text{CH}_3$  and  $\text{CH}_2$  bending vibrations in CaO/CNC, which are in the range of 1450–1300  $\text{cm}^{-1}$ . These all provide confirmation that the CaO/CNC composite was successfully formed.

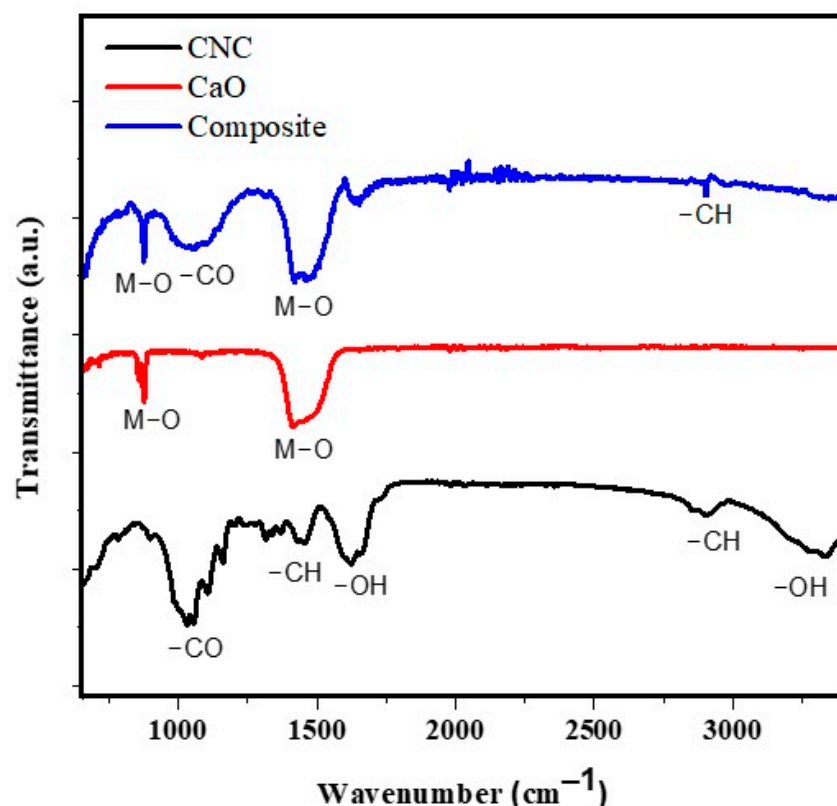


**Figure 2.** FT-IR spectra of CaO, CNCs, and composite CaO/CNC.

#### 2.1.3. SEM and EDX

Scanning Electron Microscopy (SEM) and EDX for elemental analysis were used to examine the surface morphology of the produced materials including CaO, CNC, and CaO/CNC, as shown in Figure 3. Because of their polarity and electrostatic attraction, CaO nanoparticles have a smooth, regular, and flower-like appearance in their micrographs (Figure 3a,b). The CNC micrographs exhibit agglomeration and spherical particles (Figure 3c,d). Because of the presence of CaO and CNC, the composite displays porous nanoflakes and agglomerated particles of various sizes (Figure 3e,f). CaO, CNC, and CaO/CNC composite elements underwent EDX investigation. The purity of CaO NPs and the existence of C and O in cellulose are both confirmed by the presence of Ca and O in CaO nanoparticles. The presence of Ca, O, and C in the EDX spectrum effectively verifies the production of the composite CaO/CNC (Figure 4).

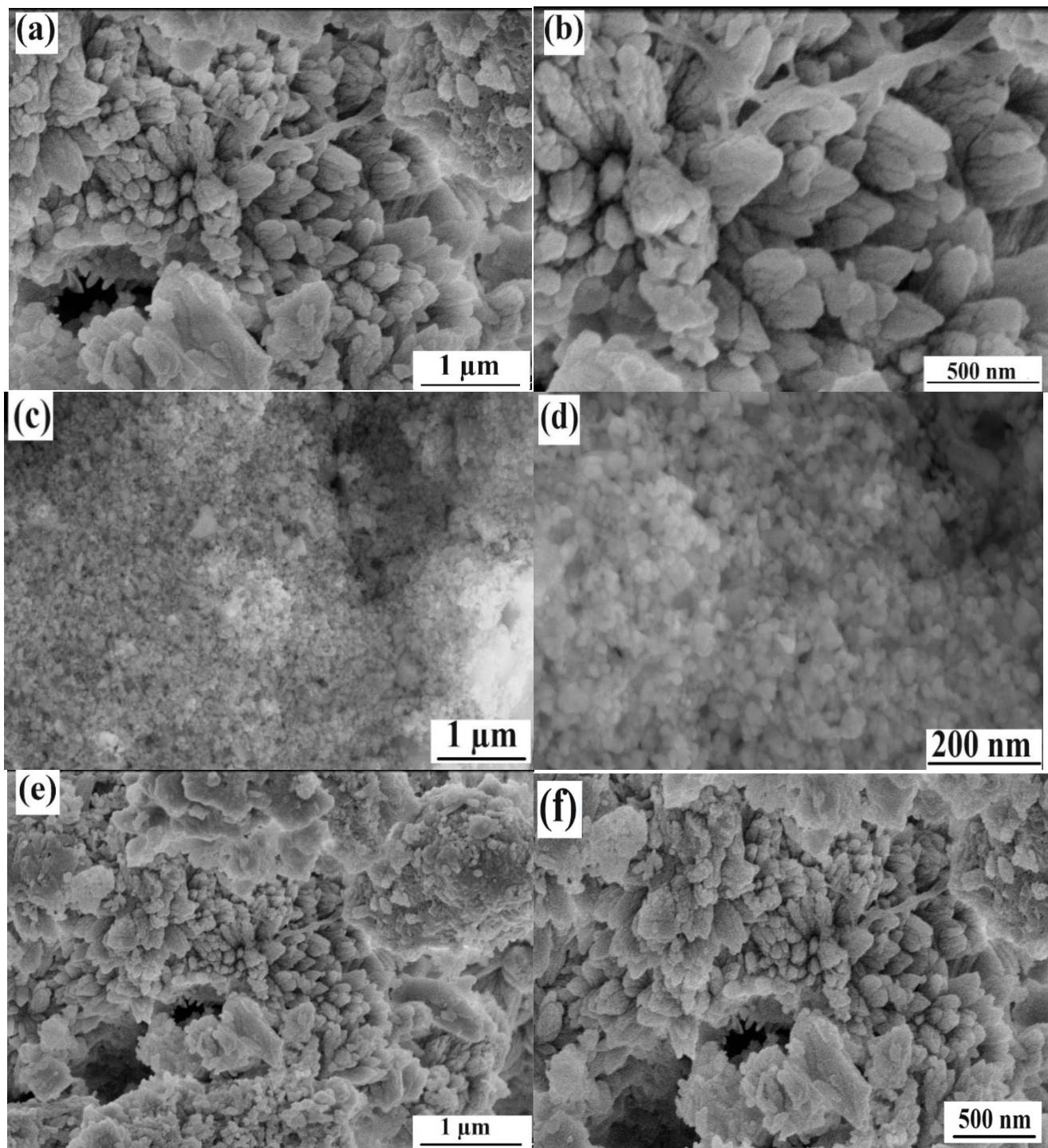


**Figure 3.** SEM images of (a,b) CaO, (c,d) CNCs, and (e,f) composite CaO/CNC at different resolutions.

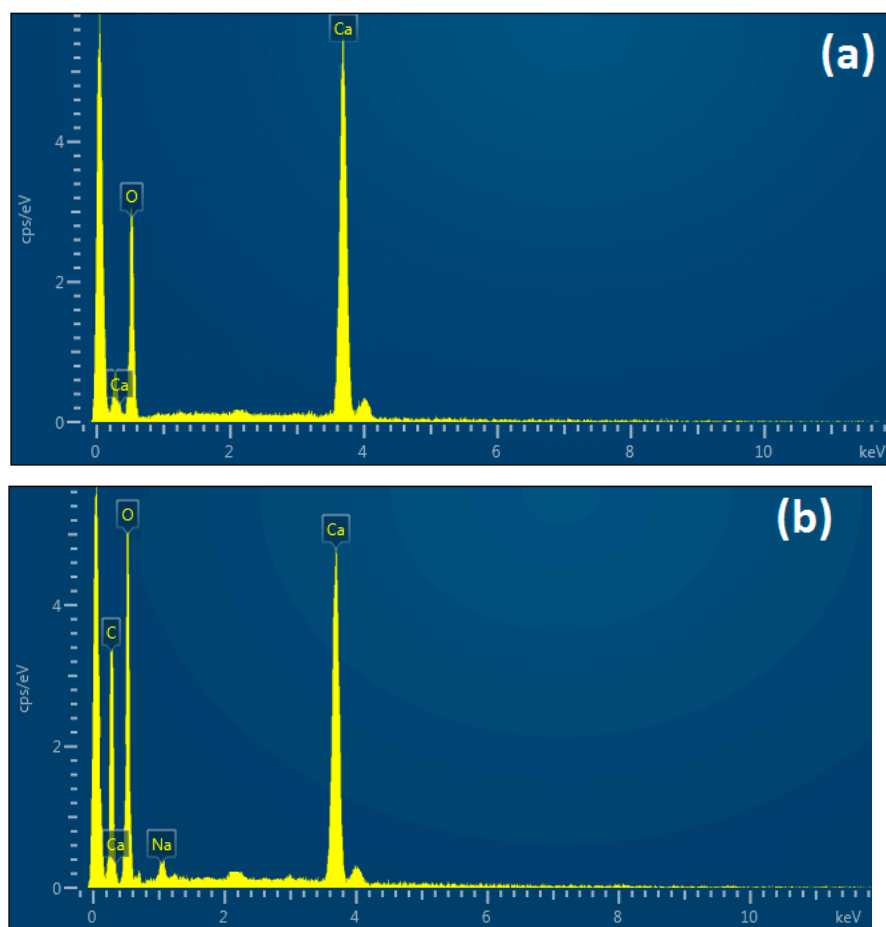


**Figure 4.** Scanning electron microscopy and energy dispersive X-ray spectroscopy of (a) CaO and the (b) CaO/CNC composite.

## 2.2. Effective Parameters of WCO Conversion to Biodiesel

To determine the impact of different effective parameters on the biodiesel yield of the used canola cooking oil, experiments were carried out three times. Temperature (50–100 °C), oil-to-methanol ratios (1:5–1:25), reaction time (30–150 min), and catalyst loading (1–5%) were the variables. The data were graphed to examine the effects of the various parameters on biodiesel yield.

### 2.2.1. Impact of Reaction Temperature

Temperature is an important factor in determining the conversion of triglycerides into biodiesel and affects the rate of the transesterification reaction. In Figure 5a, the impact of temperature on the catalyst's effectiveness is shown at temperatures varying between 40 and 80 °C with a MeOH: oil of 20:1, CaO/CNC amount of 3 wt.%, and the time of 120 min on biodiesel yield during the transesterification reaction of used fry cooking oil, which was investigated under reflux circumstances. The reaction temperature has a substantial impact on the biodiesel yield, as shown in Figure 5a. The initial biodiesel output was just 53% at 40 °C and 75% at 50 °C, but it grew further with just a 20 °C temperature rise and peaked at 84% at 60 °C. The biodiesel yield was lower at low temperatures because the oil viscosity was not reduced enough to allow for molecular collisions and a faster reaction rate. Hence, raising the reaction temperature is necessary for producing the maximum amount of biodiesel. A rise in temperature can accelerate the reaction rate and increase molecular collisions, which can reduce the activation energy [29]. Higher temperatures up to 80 °C are also used for WCO conversion to FAME [30]. The fatty acids acting as a nucleophile and the increased interaction between the catalyst and protons caused by the

alcohol and mixed oxide catalyst with the alkyl group of triglycerides facilitated a higher conversion of oils to biodiesel at the reaction site. However, the biodiesel yield dropped to 75% at temperatures above 70 °C, possibly as a result of fast methanol evaporation. This pattern is consistent with our earlier observations [4,11,21]. Hence, 60 °C was determined to be the ideal temperature for subsequent tests in this inquiry.

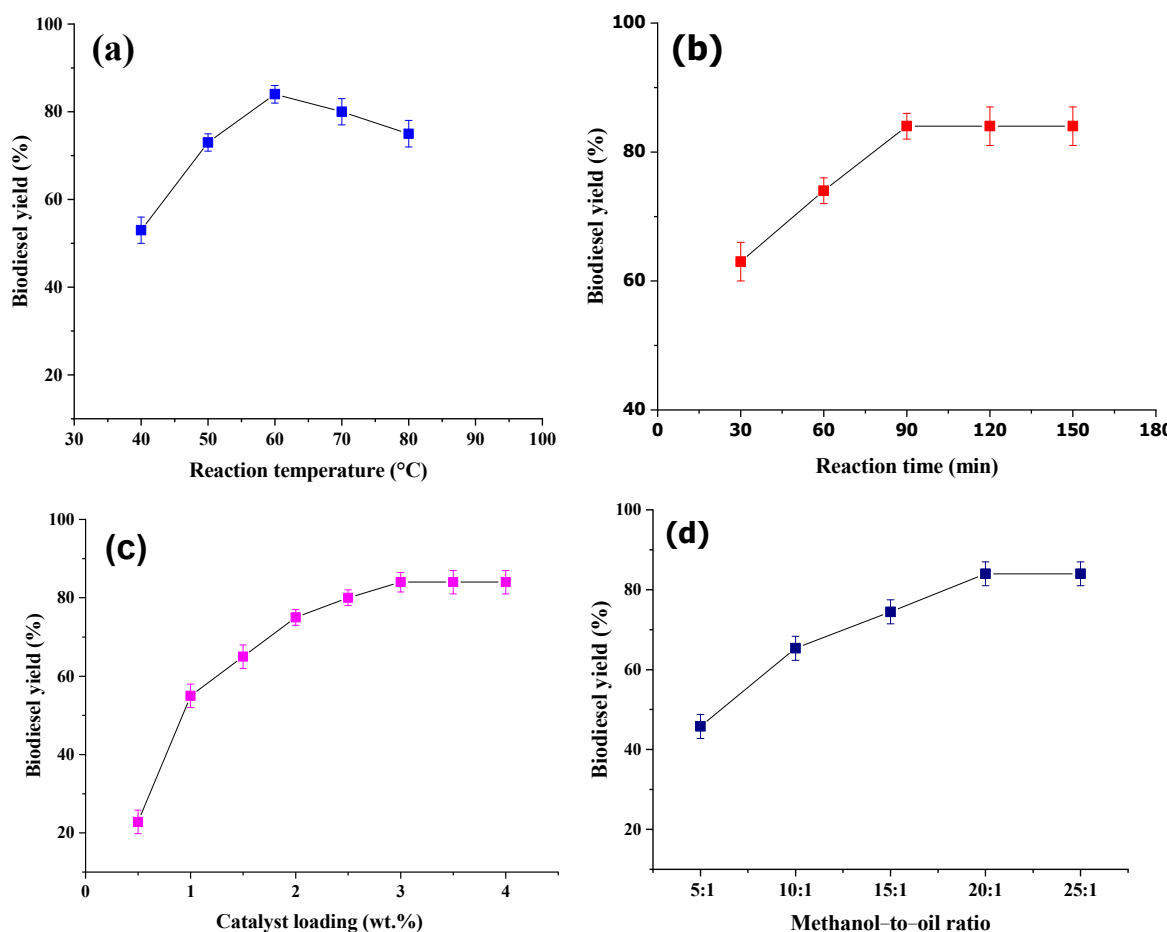


**Figure 5.** Effects of various transesterification reaction parameters on biodiesel yields: (a) reaction temperature, (b) reaction time, (c) catalyst loadings, and (d) methanol-to-oil molar ratio.

### 2.2.2. Impact of Reaction Time

The effect of transesterification reaction time on the synthesis of biodiesel from used cooking oil was investigated in this study. The 20:1 methanol-to-oil ratio, 3-weight percent catalyst loading, and reaction temperature of 60 °C were all held constant while the reaction period was changed from 30 to 150 min. The results showed that the production of biodiesel was only 63% after 30 min of reaction time (Figure 5b). The biodiesel output, however, rose as the reaction time was extended and peaked at 90 min and 84% yield. This shows that the reaction required additional time for the reactants to interact with each other and the catalyst, giving rise to higher biodiesel yield, which did not reach equilibrium after one hour. According to the present study, 90 min is the ideal amount of time for the transesterification reaction to occur. Several studies have also demonstrated that reaction time significantly affects biodiesel yield. For example, the highest biodiesel yield of 95% was attained when coconut waste oil was used as the feedstock for biodiesel synthesis by in situ transesterification using polymer-supported CaO/PVA of 2.29 wt.% and a time duration of 180 min [21]. According to earlier studies, the output of biodiesel increased as the reaction time was increased from 1 to 4 h [9,21,31]. In previous studies on the conversion of biodiesel, large reaction times were also reported ranging from 5 to 10 h [10,30,32,33].

### 2.2.3. Impact of Catalyst Loading

For transesterification processes, the involvement of the catalyst dose is crucial to produce biodiesel with a sufficient yield and quality. This study assessed the impact of catalyst loadings (1–5 wt.%) on the biodiesel yield from used cooking oil. As shown in Figure 5c, when the methanol-to-oil ratio was held at 20:1 and the reaction temperature was maintained at 60 °C for 90 min, the results showed that the lowest catalyst concentration (1%) only produced 55% biodiesel, but increasing the catalyst loading (3 wt.%) resulted in an increase in the yield by up to 84%. It was claimed earlier that at a lower catalyst concentration (ca. 0.5%), the active sites necessary to successfully convert triglycerides into biodiesel might not be present. It was discovered that using a 3 wt.% catalyst was best for producing biodiesel because of a higher number of available active sites [10]. Previous studies conducted by [31] showed that a catalyst amount of 5 wt.% could be used to convert marine fish waste oil to biodiesel. The maximum biodiesel yield of 86.5 wt.% was obtained with a methanol-to-oil molar ratio of 25:1 and a reaction time of 107 min [31]. Previously reported studies show the use of a large amount of catalyst loading, for example, a ZrO<sub>2</sub>-supported heterogeneous catalyst of 12 wt.% showed a microwave-assisted conversion of soybean oil into biodiesel yield of up to 92.75% [34]. In another study, calcined salmon fish bone waste was used as a catalyst support for biodiesel production using sunflower oil. A catalyst loading of 10 wt.% was used for 3 h to obtain a biodiesel yield of 99.13% [35]. A pyrolytic rice straw ash supported with CaO (25–35 wt.%) using a catalyst loading of 4.87 wt.% and 175 min of reaction time resulted in a biodiesel yield of 96.49% [36]. It should be noted that these amounts are considerably higher than the optimal 3 wt.% catalyst loading obtained in this research. After careful consideration, we determined that the optimal conditions for further investigation were a catalyst concentration of 3 wt.% and a MeOH: oil ratio of 20:1.

### 2.2.4. Impact of the Methanol-to-Oil Ratio

The methanol-to-oil molar ratio also affects the transesterification of used cooking oil into biodiesel using a CaO/CNC catalyst. Various methanol-to-oil ratios of 5:1, 10:1, 20:1, and 25:1 were used. We maintained a univariate approach throughout the procedure, including a catalyst loading of 3 wt.%, a reaction temperature of 60 °C, and a reaction time of 90 min. A higher methanol-to-oil ratio was used earlier in many studies, for example, a maximum biodiesel yield of 86.5 wt.% was obtained with a methanol-to-oil molar ratio of 25:1 and reaction time of 107 min [31]. Excess methanol, however, enhances the transesterification procedure on the product side, leading to a full conversion of the reactants (used cooking oil) into products (FAMEs). Figure 5d shows the effects of various methanol-to-oil molar ratios on biodiesel production. Biodiesel yields climbed from 44% to a maximum of 84% as the methanol-to-oil ratio rose from 5:1 to 20:1. This is because higher methanol-to-oil ratios make the reactants more soluble, which raises the likelihood that methanol will attack the carbonyl/carboxylic acid functional groups in fatty acids and triglycerides through a nucleophilic attack. However, when the MeOH: oil ratio was raised to 20:1 and 25:1, the biodiesel yield remained the same. As a result, for further research, we determined that the optimal ratio is MeOH-to-oil at 20:1.

## 2.3. Biodiesel Characterization

### 2.3.1. FTIR Analysis

The identification of chemical bonds and functional groups in oil and biodiesel is carried out using this excellent method of analysis. Peaks are attained in the 400 to 4000 cm<sup>-1</sup> range. The chemical structures of the FTIR spectra of the waste cooking oil and waste cooking oil biodiesel results are similar (Figure 6). However, small differences are observed in the intensities and frequencies of the absorption bands [4,9]. The presence of fatty acid methyl esters is responsible for the following peaks in waste cooking oil: 3006.9 cm<sup>-1</sup> (sp<sub>2</sub> C–H stretch), 2921.7 cm<sup>-1</sup> (sp<sub>3</sub> C–H stretch), 1377.1 cm<sup>-1</sup> (CH<sub>3</sub> bending), 1463.7 cm<sup>-1</sup> (CH<sub>2</sub> bending), 1098.6 cm<sup>-1</sup> (C–C stretch), and 1743.6 cm<sup>-1</sup> (C=O stretch).

With some small variations, similar peaks were seen in the produced biodiesel. It is notable that the methyl ester deformation peak, which appears at  $1435.5\text{ cm}^{-1}$  in the spectrum of biodiesel, is absent from the oil spectrum, which is the methyl ester group with its deformation vibration. In addition, the biodiesel spectrum's fingerprint area peak at  $1157.8\text{ cm}^{-1}$  was divided into two peaks at  $1170.3$  and  $1195.7\text{ cm}^{-1}$ . The averaging of the energy over the triple ester group of the triglycerides is gone, which strongly supported the manufacture of biodiesel. These vibrational bands show that the heterogeneous catalytic transesterification event, which turns oil into biodiesel, has taken place.

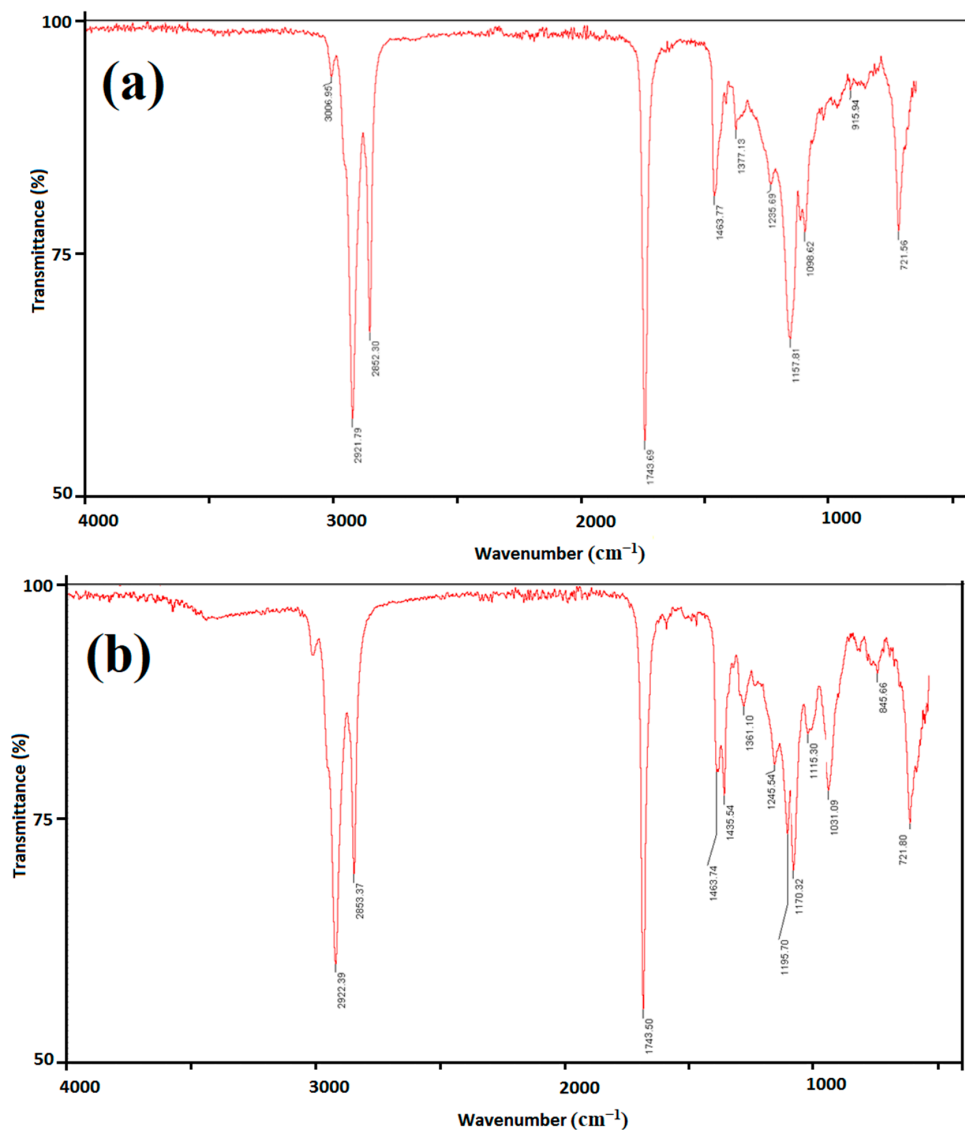


**Figure 6.** FTIR spectra of waste cooking oil (a) and biodiesel from waste cooking oil (b).

### 2.3.2. Nuclear Magnetic Resonance Analysis

$^1\text{H}$  NMR was employed to determine the molecular composition of biodiesel, which is also used to demonstrate that methyl ester was produced during the transesterification procedure. The Figure 7a depicts the biodiesel  $^1\text{H}$  NMR spectrum and its associated signals. The signal that appeared at 0.89 ppm is attributed to terminal methyl protons ( $\text{C}-\text{CH}_3$ ), at 1.32–1.95 ppm to methylene groups ( $\alpha-\text{CH}_2$ ,  $\beta-\text{CH}_2$ ), which suggested the existence of hydrogen atoms on the third carbon in an aliphatic fatty chain, and at 2.27 ppm to methylene protons ( $\text{C}-\text{CH}_3$ ). The signal at 0.87 ppm is attributed to terminal methyl protons, while the peak of olefinic hydrogen ( $-\text{CH}=\text{CH}-$ ) appears at 5.37 ppm, signifying

the double bond integrated for two hydrogen atoms for each double bond group. The spectra peak at 2.32 ppm is for allylic hydrogen ( $-\text{CH}_2-$ ), which has two hydrogen atoms per non-conjugated group. The appearance of a peculiar single peak at 3.6 ppm, which is attributed to methoxy protons ( $-\text{OCH}_3$ ), is evidence of the production of methyl esters. Figure 7b illustrates the  $^{13}\text{C}$  NMR spectra, demonstrating distinctive signals at 31.91 ppm and 174.25 ppm that are related to ( $-\text{CH}_2-$ )<sub>n</sub> and ( $-\text{COO}-$ ), respectively. The unsaturated position in biodiesel ( $\text{CH}=\text{CH}$ ) methyl ester was detected at 129.7 ppm for outer non-conjugated carbon. The conversion of oil into biodiesel was also confirmed by employing the following formula, as reported elsewhere [13,37,38]:

$$C = 100 \times \frac{2A(\text{Me})}{3A(\text{CH}_2)}$$

The above equation, where  $C$ ,  $A(\text{Me})$ , and  $A(\text{CH}_2)$  are the percentage conversion, integration values of methoxy protons, and alpha methylene proton, respectively, was used to calculate the biodiesel yield from waste cooking oil. The conversion of WCO to biodiesel was obtained as 82.8% by using the above formula, which is quite close to the practically obtained yield of 84%.

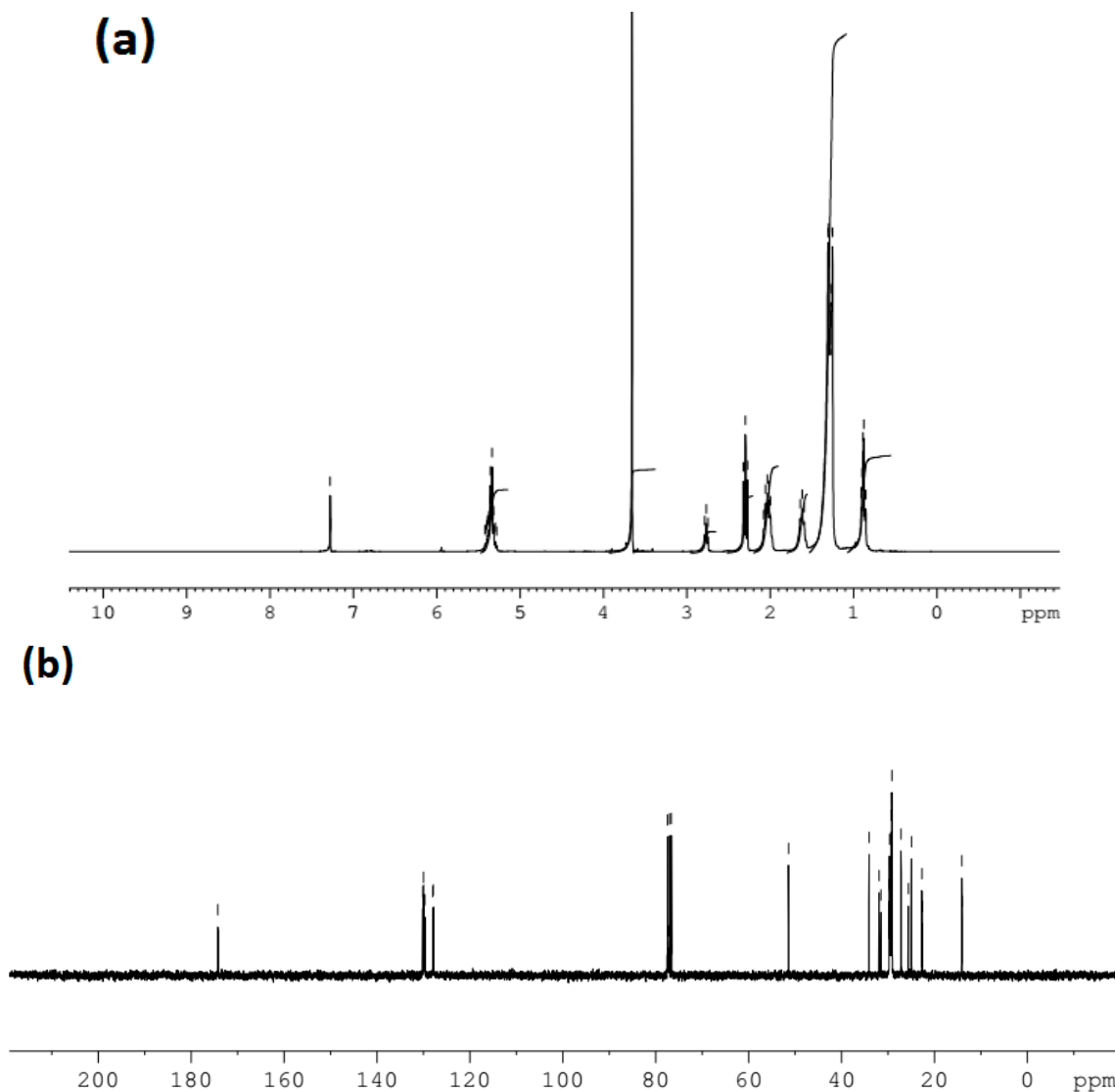


**Figure 7.** NMR spectra of (a)  $^1\text{H}$  and (b)  $^{13}\text{C}$  for biodiesel produced from waste cooking oil.

### 2.3.3. GC-MS Analysis

The produced biodiesel from the waste cooking oil chemical composition was analyzed further by GC-MS (Figure 8). The analysis of the biodiesel samples using library software (NO. NIST02) allowed for the identification of various FAMEs (fatty acid methyl esters). The mass spectra of docosanoic methyl ester ( $C_{22}:0$   $m/z$  354) appeared at a retention time of 15,611 min and octadecanoic acid methyl ester ( $C_{18}:0$   $m/z$  298) at a 12,177 min retention time, which is saturated fatty acid methyl ester. The mass spectrum shows important fragment ions characteristic of monosaturated fatty acid methyl esters such as tetracosenoic acid methyl ester ( $C_{25}:0$ ,  $m/z$  382) and other saturated fatty acid methyl esters including eicosanoic acid methyl ester ( $C_{21}:0$ ,  $m/z$  326), hexadecanoic methyl ester ( $C_{17}:0$ ,  $m/z$  270), and methyl tetradecanoate ( $C_{15}:0$ ,  $m/z$  242). Moreover, other monounsaturated fatty acid methyl esters were also observed, such as 10-octadecenoic acid methyl ester ( $C_{10}:1$ ) and 11-eicosenoic acid methyl ester ( $C_{21}:1$ ) at  $m/z$  324 and  $m/z$  296. Furthermore, the current peaks exhibited saturated and unsaturated McLafferty rearrangements ( $m/z = 74$  and  $29$ ). The fatty acid methyl ester profile is the key factor in determining feedstock's suitability in synthesizing biodiesel. However, it should be noted that the presence of a higher degree of unsaturated fatty acids can limit the suitability of (FAMEs) fatty acid methyl esters as fuel because of issues such as peroxidation and polymerization. Peroxidation occurs at an accelerated rate in combustion engines at higher temperatures, which can lead to engine clogging. As a result, feedstocks with a higher proportion of polyunsaturated fatty acids are not ideal for biodiesel production. Conversely, monounsaturated acids have a lower affinity for oxygen, minimizing the risk of peroxidation [39,40].

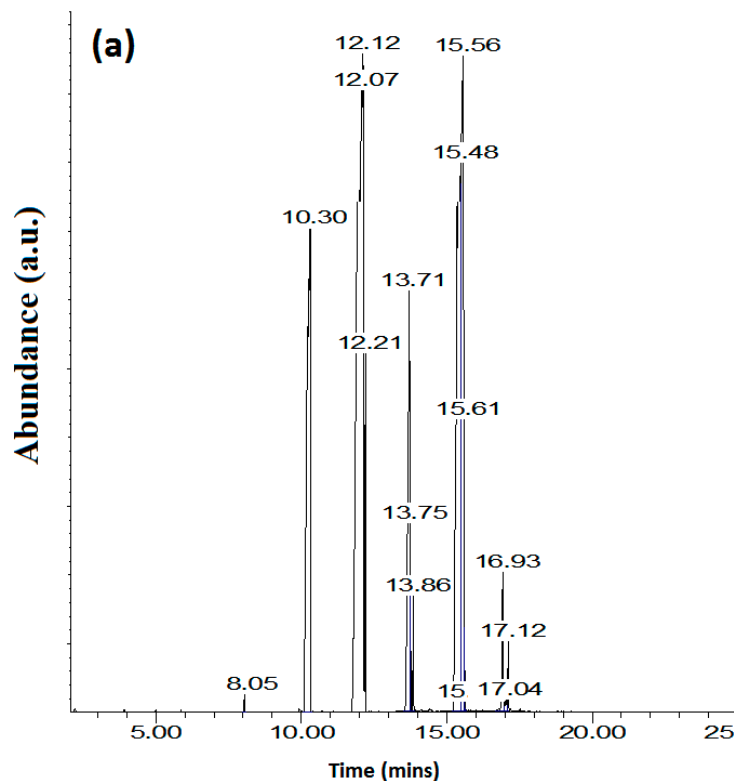
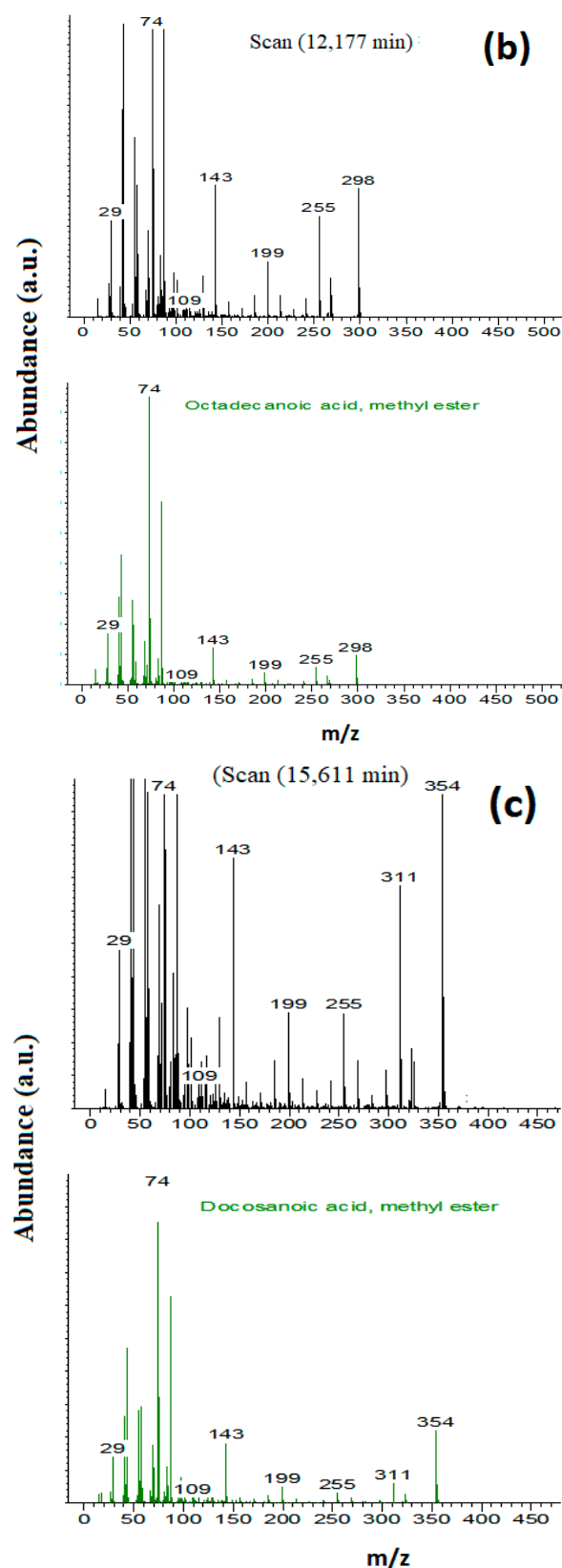


Figure 8. Cont.



**Figure 8.** GC-MS chromatograms. (a) Total ion chromatogram of biodiesel, (b), Library match of peak at 12,177 min (octadecanoic acid methyl ester ( $C_{18}:0$ )), and (c) Library match of peak at 15,611 (docosanoic methyl ester ( $C_{22}:0$ ))).

#### 2.4. Comparison of Biodiesel Fuel Properties with International Standards

As recommended by ASTM, the fuel qualities of the synthesized biodiesel were evaluated. The test findings are consistent with international standards, including those indicated in Table 1 such as ASTM-951, 6751, Chinese international standards (GB/T 20828), and European Union standards (EU-14214). To establish the coherence of the synthesized biodiesel's properties with slight alterations, it was compared with earlier research. Higher acid numbers result in engine damage and poorer engine efficiency, and there is a correlation between the acid number and the level of free fatty acids (FFAs) in the fuel. Nonetheless, the synthetic biodiesel is within the permitted range for international standards with an acid value of 0.31 mg KOH/g. High-density fuels can contribute to engine viscosity issues and have an impact on atomization during combustion. For FAMEs, the density should be between 860 and 900 kg/m<sup>3</sup>, as mandated by American (ASTM) and European (EU) requirements, which is somewhat higher than that of petro-diesel density (827.2 kg/m<sup>3</sup>) [41,42]. This research discovered that the produced biodiesel's density was 0.8312 kg/m<sup>3</sup>, which is within the bounds established by international regulations (Table 1). This shows that switching to biodiesel as a diesel fuel substitute will not have any negative consequences on the engine or the environment. We also examined kinematic viscosity, a fundamental property of biodiesel that is impacted by fuel spray, mix formation, and combustion. It is crucial to keep the kinematic viscosity as low as possible because high viscosity can cause deposits to build up and poor combustion in the engine. It was discovered that the kinematic viscosity of the biodiesel made from used cooking oil was 5.88 centistokes (cSt) (Table 1), which is slightly higher than the values discovered in prior research utilizing seed oils from the rubber raphnus L. and jatropha (5.65, 5.65, and 4.36 cSt, respectively) [10]. The biodiesel used in the current experiment has a flash point of 77 °C, which is within the permissible range for fuels with flash points higher than 66 °C, as defined by American (ASTM), Chinese (PRC), and European Standards (EU). That is, however, still below the targeted cap. The term "flash point" describes the temperature at which fuel begins to vaporize and catch fire when exposed to a spark [10].

**Table 1.** Comparison of fuel properties of the waste cooking oil biodiesel with international biodiesel standards and biodiesel from other studies.

Parameters	Unit	Test Method	Typical Values of Diesel (Market)	Observed Values
Specific gravity (15.6 °C)	No unit	ASTMD1298	<0.860	0.904
Color	No unit	ASTMD1500	Min. 3	4
Flash point	°C	ASTM D93	Min. 54	77
Cloud point	°C	ASTMD2500	Max. 9	-3
Pour point	°C	ASTM D97	Max. 9	-5
Viscosity (kinematic at 50 °C)	cSt or mm <sup>2</sup> /s	ASTM D445	Max. 12	5.88
Sulfur	wt.%	ASTMD4294	Max. 1.8	0.0001
Sediments	wt.%	ASTM D473	Max. 0.05	0.014
Water content	wt.%	ASTM D95	Max. 0.25	0.046
Total acid number	mg KOH/gm	ASTM D664	Max. 0.5	0.31
Cetane number	No unit	ASTM D976	Min. 35	29
Copper strip (3 h corrosion at 100 °C)	No unit	ASTM D130	Max. 1	1a

## 2.5. Reusability of Catalyst

The reusability of the CaO/CNC catalyst's efficacy was assessed to evaluate the stability of nanocomposite in the transesterification of biodiesel production under optimal reaction conditions. The optimized transesterification reaction conditions, which included a 3-weight percent catalyst loading, a 20:1 methanol-to-oil ratio, a reaction temperature of 60 °C, and a 90-min reaction period, were employed to test the catalytic activity of the recycled catalyst. Up to five times reusability was possible for the catalyst after it was removed from the reaction mixture. The separation and cleaning procedure reduced the catalyst activity of the regenerated catalyst. After each process, the used catalyst was collected using filter paper, cleaned with methanol to remove any contaminants, and then utilized in tests on catalyst leaching. The catalyst activity in the following five reactions was assessed after the catalyst surface had completely dried at 100 °C for at least three hours. It was noted that throughout the three recycling procedures, the biodiesel yields fell somewhat from 84% to 82%. The biodiesel efficiency declined because of the leaching effect of active species in the reaction mixture after frequent use. In addition, CaO nanoparticles contained in the reaction can be solubilized in the glycerol attained by way of a by-product, i.e., calcium diglyceroxide species, which is the active phase in biodiesel manufacture [43]. The deactivation of catalytic active sites resulted in a further decline in biodiesel yields after each run, which explained why they reached 79% in the fifth cycle (Figure 9). However, the potentiality of the prepared nanocatalyst to be reused in biodiesel production can reduce the raw material cost of the overall production [44]. In a similar study [21], the yield of biodiesel was reduced from 94.55% to 67.07% after five cycles, and the pattern in terms of catalyst reusability was similar to the current study, where the yield of biodiesel was decreased slightly at the early cycle. The comparison between the CaO/CNC composite and pristine CaO was made using the same reaction conditions (Figure 9), and it was observed that the composite shows a better reaction rate and stability compared with pristine CaO. The reaction kinetics of pristine CaO is quite slow and takes time, which limits its suitability to be used as a catalyst. For this reason, researchers used modifications/doping or composite formation to enhance the reaction rates of CaO [20]. For example, Tang et al. modified CaO by treating it with bromooctane and obtained a lower reaction time of 3 h (99.2% conversion) compared with CaO (35.4% conversion) [19].

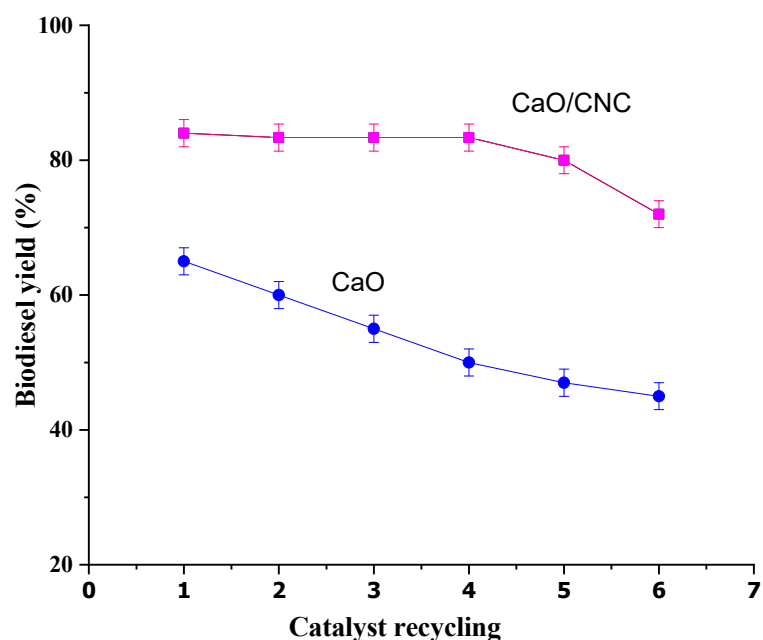


**Figure 9.** Recycling of CaO/CNC nanocomposite and CaO during transesterification reactions.

### 3. Materials and Methodology

#### 3.1. Materials

The chemicals, which were used at analytical grade, came from Sigma Aldrich. These included sodium hydroxide ( $\text{NaOH}$ ), calcium nitrate hexahydrate ( $\text{Ca}(\text{NO}_3)_2 \cdot 6\text{H}_2\text{O}$ ), hydrochloric acid ( $\text{HCl}$ ), methanol ( $\text{CH}_3\text{OH}$ ), sulfuric acid ( $\text{H}_2\text{SO}_4$ ), ethanol ( $\text{C}_2\text{H}_5\text{OH}$ ), anhydrous magnesium sulfate ( $\text{MgSO}_4$ ), and filter paper (No 41). Vegetable oil, canola waste cooking oil (WCO), was obtained from a nearby local restaurant.

#### 3.2. Cellulose Nanocrystal Synthesis (CNC)

The world's most prevalent and renewable biopolymer is cellulose, which is derived from renewable resources like biomass [45]. Nanocrystalline cellulose (CNC) has a strong crystalline structure, is densely packed, inexpensive, and lightweight, and has distinct morphologies with nanoscale dimensions [46]. Acid hydrolysis was carried out under regulated conditions to separate the CNCs, ensuring that only the amorphous segments of the cellulose were acted on and the crystalline segments were left unaltered. Sulfuric acid and hydrochloric acid are the most often used acids for the acid hydrolysis of cellulose because of their considerable strength, which is necessary to hydrolyze the glycosidic link present in cellulose [47]. In fact, exposing cellulose fibers to acid hydrolysis can produce defect-free, rod-like crystalline residues [47]. The structure of cellulose is supramolecular, and acid hydrolysis causes a certain degree of cellulose structure breakage, resulting in lower molecular weight constituents and molecular weight distribution with smaller molecular fractions [48,49]. CNC was fabricated using acid hydrolysis of filter paper No 41, which is a cheap and easily available source of cellulose, requiring less effort and purification steps than other raw sources of cellulose. A homogenous suspension of 2 g of filter paper was prepared by cutting, pulverizing, and dissolving it in a 62%  $\text{H}_2\text{SO}_4$  acid solution. The mixture was then placed in a water bath at 45 °C and continuously stirred for an hour. The addition of adequate DI water stopped hydrolysis (20-fold), and then the acid was neutralized to stop the hydrolysis process. The excess water was removed, and sediments were collected using centrifuging at  $8000 \times g$  rpm for 15 min. Thereafter, the suspension was cleaned several times with deionized water (DI) water. The total solid content of CNC was determined by drying at 100 °C for 1 h.

#### 3.3. $\text{CaO}/\text{CNC}$ Nanocomposite

In the current experiment, pure calcium oxide ( $\text{CaO}$ ) nanoparticles were produced by the direct precipitation method, which is one of the most useful, budget-effective, easy, and traditional methods, following the steps reported previously with some modifications [50].  $\text{Ca}(\text{NO}_3)_2 \cdot 6\text{H}_2\text{O}$  was properly weighed out and dissolved in (100 mL) distilled water at 60 °C under constant stirring for 1 h using a hotplate magnetic stirrer. A solution of  $\text{NaOH}$  (1 M) prepared in distilled water was added dropwise into the  $\text{Ca}(\text{NO}_3)_2 \cdot 6\text{H}_2\text{O}$  solution (40 mL). The reaction process was carried out for 2 h at a temperature of 60 °C and  $\text{pH} = 10$ , which resulted in white-colored precipitates. These precipitates were filtered and washed with ethanol and distilled water. The end product of this chemical reaction was a precursor of  $\text{CaO}$ , that is,  $\text{Ca}(\text{OH})_2$ , and dried in an oven for 6 h at 60 °C, which was finally calcinated at 900 °C for 5 h.

$\text{CaO}/\text{CNC}$  nanocomposites were synthesized by the hydrothermal method. Separately, 1 g of CNC and 1 g of calcium oxide nanoparticles were added to 40 mL of 96% ethanol, which was then sonicated for 30 min separately to attain good dispersion. The solutions were slowly combined and sonicated for five minutes and then transferred to an autoclave Teflon for 12 h at 120 °C. The resulting product was centrifuged, dried at 60 °C overnight, and used for transesterification reaction.

#### 3.4. Free Fatty Acid Content (FFA) Determination of WCO

It is essential to know the FFA content of the oil sample before transesterification. The acid–base titration method was used to determine the level of FFA in the used cooking oil.

Two grams of WCO was added in a 250 mL titration flask, and 100 mL of solution was prepared by adding ethanol–diethyl ether (1:1 *v/v*) by using a few drops of phenolphthalein added in the sample solution as an indicator and titrated with standardized potassium hydroxide 0.025 M solution. Using the following equation, the FFA content of the used cooking oil was determined [51]:

$$\% \text{FFA} = \frac{V \text{ (mL)} C \times M \times 100}{1000 \times m \text{ (gram)}}$$

where *V* is the volume of oil/solvent solution, *C* is the concentration of KOH in molarity, *M* is the molecular weight of oleic acid (most commonly used fatty acid), and *m* is the mass of oil used. A free fatty acid content of 3.5% was found in the waste cooking oil.

### 3.5. Process of Biodiesel Production

The presence of FFAs in biodiesel reduces its commercial value. As per international biodiesel standards, an acid number of less than 0.5% (mg KOH/g) is recommended. Therefore, after determining the acid value and FFA content of the WCO, acid esterification via pre-treatment was conducted to reduce its FFA content. In this study, the pre-treatment was performed using the conventional oil bath method. A three-necked round-bottom flask was utilized for the pre-treatment process. A reflux condenser was connected to the top neck of the flask to reduce the evaporative loss of alcohol, while the left neck was connected to a thermometer to measure the temperature. The right neck was closed with a stopper to reduce the evaporative loss of alcohol [52]. This was accomplished by an esterification process using cooking oil that was first filtered using a filter strainer to remove impurities. The methanol and oil were then mixed in a 2:1 molar ratio with 5 wt.% of HCl and 60 mL of WCO added. This mixture was then stirred for one hour at 60 °C on a reflux condenser. Distilled water was then added (50–100 mL) and repeatedly rinsed to remove unreacted acid and any other side products. The remaining oil phase was treated with MgSO<sub>4</sub> for 30 min until all the water in the oil was dried.

After the esterification of FFAs in the waste cooking oil was reduced to less than 0.5%, the CaO/CNC catalyst was used to produce biodiesel from esterified waste cooking oil. The transesterification reaction was performed using 30 mL of esterified oil for 90 min at 60 °C with a methanol-to-oil molar ratio of 20:1 and 3% CaO/CNC catalyst. Biodiesel and glycerol were produced during the transesterification reaction. Excess methanol was evaporated using a rotary evaporator, and the glycerol and biodiesel layers were separated using a separating funnel. The yield of biodiesel was estimated using the following equation, as per previously reported studies [11,13,30]:

$$\text{Percentage yield} = \frac{\text{Grams of Biodiesel Produced}}{\text{Grams of Oil Used}} \times 100$$

### 3.6. Instrumentation

Powder X-ray diffraction (PXRD) is a crucial technique for identifying the crystalline phases present in materials and for determining the structural properties. PXRD patterns of CaO, CNCs, and CaO/CNCs composite were obtained using a powder diffractometer (Model X'Pert powder X-ray diffractometer from PANalytical) equipped with a Cu-K $\alpha$  radiation detector with a wavelength of 0.154 nm and a scanning rate of 2°/min in the 2θ range of 10–70°. The Scherrer equation, which relates the average crystallite size (*D*) to the diffraction width ( $\beta$ ), was used to determine the crystallite size based on the broadening of the relevant X-ray spectral peaks. The Scherrer equation and the full-width half maximum (FWHM) of the sharpest peak were used to determine the crystallite sizes.

$$D = K \cdot \lambda / (\beta \cdot \cos \theta)$$

where *D* = Diameter of crystallite;

$K$  = Shape factor, having a value of 0.9;

$\lambda$  = Wavelength of the incident X-ray, having a value of 1.542 Å;

$\beta$  = Full-width half maxima of the corresponding diffraction peak;

$\theta$  = Bragg's angle.

Functional groups and the bond formation of materials were studied by FT-IR (BRUKER-TENSOR-27) in the range of  $4000\text{ cm}^{-1}$  to  $400\text{ cm}^{-1}$  with a resolution rate  $1\text{ cm}^{-1}$  and 15 scans. Scanning electron microscopic study by NOVA Nano exposed the surface morphology (shape and size) and elemental analysis via energy-dispersive X-ray spectroscopy (EDX).

#### 4. Conclusions

In this study, an efficient heterogeneous catalyst CaO/CNC nanocomposite is used for the transesterification of waste cooking oil. Filter paper is used as a cheap source for the development of CNCs, which typically possesses a high surface area and porosity. The filter paper can be replaced in the future with a cheap source of lignocellulosic biomass available abundantly for CNC preparation. The CaO/CNC nanocomposite possesses more active sites, which enhance the efficiency of the transesterification. The hydrothermally synthesized CaO/CNC composite is employed as a catalyst to synthesize biodiesel through transesterification, which is confirmed by different characterizations including XRD, SEM, and EDX. The impact of different operating conditions on the production of biodiesel was investigated thoroughly, such as a molar ratio of methanol-to-oil of 20:1, catalyst concentration (3 wt.%), temperature ( $60\text{ }^{\circ}\text{C}$ ), and time (90 min). Under these optimum conditions, a biodiesel yield of 84% was obtained. The CaO/CNC catalyst can be recycled up to five times without significantly lowering conversion efficiency and shows good stability compared with pristine CaO. To confirm the successful transesterification process, various analytical techniques such as  $^{1}\text{H-NMR}$ ,  $^{13}\text{C-NMR}$ , GC-MS, and FT-IR spectroscopy were employed. The physicochemical characteristics evaluated in this study unequivocally demonstrate that waste cooking oil has the potential to serve as a valuable non-edible feedstock for the biodiesel industry. Its economic feasibility, local availability, environmental friendliness, and adaptability to diverse environmental conditions make it a promising candidate for sustainable biodiesel production. The properties of the biodiesel, such as cetane number, kinematic viscosity, flash point, copper strip corrosion, and water content, align with international standards. These biodiesel properties also meet the standards set by China, the European Union, and the United States. Consequently, biodiesel can be considered a compelling substitute for petroleum diesel. This research offered a cheap and environmentally beneficial technique for synthesizing biodiesel with high yield.

**Author Contributions:** Data curation, M.R., M.S. and S.D.A.; formal analysis, S.K.; funding acquisition, A.A.; investigation, S.K.; project administration, A.W.; resources, M.S. and A.A.; software, M.R. and S.D.A.; supervision, A.W.; writing—original draft, S.K.; writing—review and editing, A.W. All authors have read and agreed to the published version of the manuscript.

**Funding:** The researchers would like to thank the Deanship of Scientific Research, Qassim University, Saudi Arabia, for funding the publication of this project.

**Data Availability Statement:** The authors confirm that the data supporting the findings of this study are available within the article.

**Conflicts of Interest:** The authors declare that they have no known competing financial interests or personal relationships that could have appeared to influence the work reported in this paper.

## References

- Moradi, P.; Saidi, M. Biodiesel production from Chlorella Vulgaris microalgal-derived oil via electrochemical and thermal processes. *Fuel Process. Technol.* **2022**, *228*, 107158. [[CrossRef](#)]
- Osman, A.I.; Chen, L.; Yang, M.; Msigwa, G.; Farghali, M.; Fawzy, S.; Rooney, D.W.; Yap, P.-S. Cost, environmental impact, and resilience of renewable energy under a changing climate: A review. *Environ. Chem. Lett.* **2023**, *21*, 741–764. [[CrossRef](#)]
- Osman, A.I.; Elgarahy, A.M.; Eltaweil, A.S.; Abd El-Monaem, E.M.; El-Aqapa, H.G.; Park, Y.; Hwang, Y.; Ayati, A.; Farghali, M.; Ihara, I.; et al. Biofuel production, hydrogen production and water remediation by photocatalysis, biocatalysis and electrocatalysis. *Environ. Chem. Lett.* **2023**, *21*, 1315–1379. [[CrossRef](#)]
- Jabeen, M.; Munir, M.; Abbas, M.M.; Ahmad, M.; Waseem, A.; Saeed, M.; Kalam, M.A.; Zafar, M.; Sultana, S.; Mohamed, A.; et al. Sustainable Production of Biodiesel from Novel and Non-Edible Ailanthus altissima (Mill.) Seed Oil from Green and Recyclable Potassium Hydroxide Activated Ailanthus Cake and Cadmium Sulfide Catalyst. *Sustainability* **2022**, *14*, 10962. [[CrossRef](#)]
- Munir, M.; Saeed, M.; Ahmad, M.; Waseem, A.; Alsaady, M.; Asif, S.; Ahmed, A.; Shariq Khan, M.; Bokhari, A.; Mubashir, M.; et al. Cleaner production of biodiesel from novel non-edible seed oil (*Carthamus lanatus* L.) via highly reactive and recyclable green nano CoWO<sub>3</sub>@rGO composite in context of green energy adaptation. *Fuel* **2023**, *332*, 126265. [[CrossRef](#)]
- Emmanouilidou, E.; Mitkidou, S.; Agapiou, A.; Kokkinos, N.C. Solid waste biomass as a potential feedstock for producing sustainable aviation fuel: A systematic review. *Renew. Energy* **2023**, *206*, 897–907. [[CrossRef](#)]
- Emmanouilidou, E.; Lazaridou, A.; Mitkidou, S.; Kokkinos, N.C. A comparative study on biodiesel production from edible and non-edible biomasses. *J. Mol. Struct.* **2024**, *1306*, 137870. [[CrossRef](#)]
- Osman, A.I.; Mehta, N.; Elgarahy, A.M.; Al-Hinai, A.; Al-Muhtaseb, A.A.H.; Rooney, D.W. Conversion of biomass to biofuels and life cycle assessment: A review. *Environ. Chem. Lett.* **2021**, *19*, 4075–4118. [[CrossRef](#)]
- Munir, M.; Ahmad, M.; Mubashir, M.; Asif, S.; Waseem, A.; Mukhtar, A.; Saqib, S.; Siti Halimatul Munawaroh, H.; Lam, M.K.; Shiong Khoo, K.; et al. A practical approach for synthesis of biodiesel via non-edible seeds oils using trimetallic based montmorillonite nano-catalyst. *Bioresour. Technol.* **2021**, *328*, 124859. [[CrossRef](#)]
- Munir, M.; Ahmad, M.; Rehan, M.; Saeed, M.; Lam, S.S.; Nizami, A.S.; Waseem, A.; Sultana, S.; Zafar, M. Production of high quality biodiesel from novel non-edible Raphanus raphanistrum L. seed oil using copper modified montmorillonite clay catalyst. *Environ. Res.* **2021**, *193*, 110398. [[CrossRef](#)]
- Munir, M.; Ahmad, M.; Saeed, M.; Waseem, A.; Nizami, A.-S.; Sultana, S.; Zafar, M.; Rehan, M.; Srinivasan, G.R.; Ali, A.M. Biodiesel production from novel non-edible caper (*Capparis spinosa* L.) seeds oil employing Cu-Ni doped ZrO<sub>2</sub> catalyst. *Renew. Sustain. Energy Rev.* **2021**, *138*, 110558. [[CrossRef](#)]
- Nasreen, S.; Liu, H.; Skala, D.; Waseem, A.; Wan, L. Preparation of biodiesel from soybean oil using La/Mn oxide catalyst. *Fuel Process. Technol.* **2015**, *131*, 290–296. [[CrossRef](#)]
- Munir, M.; Ahmad, M.; Saeed, M.; Waseem, A.; Rehan, M.; Nizami, A.-S.; Zafar, M.; Arshad, M.; Sultana, S. Sustainable production of bioenergy from novel non-edible seed oil (*Prunus cerasoides*) using bimetallic impregnated montmorillonite clay catalyst. *Renew. Sustain. Energy Rev.* **2019**, *109*, 321–332. [[CrossRef](#)]
- Munir, M.; Saeed, M.; Ahmad, M.; Waseem, A.; Sultana, S.; Zafar, M.; Srinivasan, G.R. Optimization of novel *Lepidium perfoliatum* Linn. Biodiesel using zirconium-modified montmorillonite clay catalyst. *Energy Sources Part A Recovery Util. Environ. Eff.* **2022**, *44*, 6632–6647. [[CrossRef](#)]
- Foroutan, R.; Peighambardoust, S.J.; Mohammadi, R.; Peighambardoust, S.H.; Ramavandi, B. Application of walnut shell ash/ZnO/K<sub>2</sub>CO<sub>3</sub> as a new composite catalyst for biodiesel generation from *Moringa oleifera* oil. *Fuel* **2022**, *311*, 122624. [[CrossRef](#)]
- Yaakob, Z.; Mohammad, M.; Alherbawi, M.; Alam, Z.; Sopian, K. Overview of the production of biodiesel from Waste cooking oil. *Renew. Sustain. Energy Rev.* **2013**, *18*, 184–193. [[CrossRef](#)]
- Atabani, A.E.; Silitonga, A.S.; Badruddin, I.A.; Mahlia, T.; Masjuki, H.; Mekhilef, S. A comprehensive review on biodiesel as an alternative energy resource and its characteristics. *Renew. Sustain. Energy Rev.* **2012**, *16*, 2070–2093. [[CrossRef](#)]
- Huaping, Z.; Zongbin, W.; Yuanxiong, C.; Zhang, P.; Shijie, D.; Xiaohua, L.; Zongqiang, M. Preparation of biodiesel catalyzed by solid super base of calcium oxide and its refining process. *Chin. J. Catal.* **2006**, *27*, 391–396.
- Tang, Y.; Xu, J.; Zhang, J.; Lu, Y. Biodiesel production from vegetable oil by using modified CaO as solid basic catalysts. *J. Clean. Prod.* **2013**, *42*, 198–203. [[CrossRef](#)]
- Al-Muhtaseb, A.A.H.; Jamil, F.; Osman, A.I.; Tay Zar Myint, M.; Htet Kyaw, H.; Al-Hajri, R.; Hussain, M.; Ahmad, M.N.; Naushad, M. State-of-the-art novel catalyst synthesised from waste glassware and eggshells for cleaner fuel production. *Fuel* **2022**, *330*, 125526. [[CrossRef](#)]
- Talha, N.S.; Sulaiman, S. In situ transesterification of solid coconut waste in a packed bed reactor with CaO/PVA catalyst. *Waste Manag.* **2018**, *78*, 929–937. [[CrossRef](#)]
- Padalkar, S.; Capadona, J.R.; Rowan, S.J.; Weder, C.; Won, Y.-H.; Stanciu, L.A.; Moon, R.J. Natural biopolymers: Novel templates for the synthesis of nanostructures. *Langmuir* **2010**, *26*, 8497–8502. [[CrossRef](#)]
- Rezayat, M.; Blundell, R.K.; Camp, J.E.; Walsh, D.A.; Thielemans, W. Green one-step synthesis of catalytically active palladium nanoparticles supported on cellulose nanocrystals. *ACS Sustain. Chem. Eng.* **2014**, *2*, 1241–1250. [[CrossRef](#)]
- Zik, N.; Sulaiman, S.; Jamal, P. Biodiesel production from waste cooking oil using calcium oxide/nanocrystal cellulose/polyvinyl alcohol catalyst in a packed bed reactor. *Renew. Energy* **2020**, *155*, 267–277. [[CrossRef](#)]

25. Besbes, I.; Alila, S.; Boufi, S. Nanofibrillated cellulose from TEMPO-oxidized eucalyptus fibres: Effect of the carboxyl content. *Carbohydr. Polym.* **2011**, *84*, 975–983. [[CrossRef](#)]
26. Habte, L.; Shiferaw, N.; Mulatu, D.; Thenepalli, T.; Chilakala, R.; Ahn, J.W. Synthesis of nano-calcium oxide from waste eggshell by sol-gel method. *Sustainability* **2019**, *11*, 3196. [[CrossRef](#)]
27. Mirghiasi, Z.; Bakhtiari, F.; Darezereshki, E.; Esmaeilzadeh, E. Preparation and characterization of CaO nanoparticles from Ca(OH)2 by direct thermal decomposition method. *J. Ind. Eng. Chem.* **2014**, *20*, 113–117. [[CrossRef](#)]
28. Wang, Z.; Ding, Y.; Wang, J. Novel Polyvinyl Alcohol (PVA)/Cellulose Nanocrystal (CNC) Supramolecular Composite Hydrogels: Preparation and Application as Soil Conditioners. *Nanomaterials* **2019**, *9*, 1397. [[CrossRef](#)]
29. Brahma, S.; Basumatary, B.; Basumatary, S.F.; Das, B.; Brahma, S.; Rokhum, S.L.; Basumatary, S. Biodiesel production from quinary oil mixture using highly efficient Musa chinensis based heterogeneous catalyst. *Fuel* **2023**, *336*, 127150. [[CrossRef](#)]
30. Al-Muhtaseb, A.A.H.; Osman, A.I.; Jamil, F.; Al-Riyami, M.; Al-Haj, L.; Alothman, A.A.; Htet Kyaw, H.; Tay Zar Myint, M.; Abu-Jrai, A.; Ponnusamy, V.K. Facile technique towards clean fuel production by upgrading waste cooking oil in the presence of a heterogeneous catalyst. *J. King Saud Univ. Sci.* **2020**, *32*, 3410–3416. [[CrossRef](#)]
31. Karkal, S.; Kudre, T. Valorization of marine fish waste biomass and Gallus Gallus eggshells as feedstock and catalyst for biodiesel production. *Int. J. Environ. Sci. Technol.* **2023**, *20*, 7993–8016. [[CrossRef](#)]
32. Olutoye, M.A.; Wong, S.W.; Chin, L.H.; Amani, H.; Asif, M.; Hameed, B.H. Synthesis of fatty acid methyl esters via the transesterification of waste cooking oil by methanol with a barium-modified montmorillonite K10 catalyst. *Renew. Energy* **2016**, *86*, 392–398. [[CrossRef](#)]
33. Ma, L.; Wei, P.; Li, J.; Liang, L.; Li, G. Synthesis of nano-crystal PVMo2W9@[Cu<sub>6</sub>O(TZI)<sub>3</sub>(H<sub>2</sub>O)<sub>6</sub>]4·nH<sub>2</sub>O for catalytically biodiesel preparation. *J. Solid State Chem.* **2024**, *329*, 124434. [[CrossRef](#)]
34. Fatimah, I.; Rubiyanto, D.; Taushiyah, A.; Najah, F.B.; Azmi, U.; Sim, Y.-L. Use of ZrO<sub>2</sub> supported on bamboo leaf ash as a heterogeneous catalyst in microwave-assisted biodiesel conversion. *Sustain. Chem. Pharm.* **2019**, *12*, 100129. [[CrossRef](#)]
35. Mohebolkhames, E.; Kazemeini, M.; Sadjadi, S. Utilization of Salmon fish bone wastes as a novel bio-based heterogeneous catalyst-support toward the production of biodiesel: Process optimizations and kinetics studies. *Mater. Chem. Phys.* **2024**, *311*, 128522. [[CrossRef](#)]
36. Saetiao, P.; Kongrit, N.; Cheng, C.K.; Jitjamnong, J.; Direksilp, C.; Khantikulanon, N. Catalytic conversion of palm oil into sustainable biodiesel using rice straw ash supported-calcium oxide as a heterogeneous catalyst: Process simulation and techno-economic analysis. *Case Stud. Chem. Environ. Eng.* **2023**, *8*, 100432. [[CrossRef](#)]
37. Gelbard, G.; Brès, O.; Vargas, R.M.; Vielfaure, F.; Schuchardt, U.F. 1H nuclear magnetic resonance determination of the yield of the transesterification of rapeseed oil with methanol. *J. Am. Oil Chem. Soc.* **1995**, *72*, 1239–1241. [[CrossRef](#)]
38. Meher, L.C.; Vidya Sagar, D.; Naik, S.N. Technical aspects of biodiesel production by transesterification—A review. *Renew. Sustain. Energy Rev.* **2006**, *10*, 248–268. [[CrossRef](#)]
39. Nomboye, A.; Hansen, A. Prediction of cetane number of biodiesel fuel from the fatty acid methyl ester [FAME] composition. *Int. Agrophysics* **2008**, *22*, 21–29.
40. Sokoto, M.; Hassan, L.; Dangoggo, S.; Ahmad, H.; Uba, A. Influence of fatty acid methyl esters on fuel properties of biodiesel produced from the seeds oil of Curcubita pepo. *Niger. J. Basic Appl. Sci.* **2011**, *19*, 81–86. [[CrossRef](#)]
41. Amenaghawon, A.N.; Obahiagbon, K.; Isesele, V.; Usman, F. Optimized biodiesel production from waste cooking oil using a functionalized bio-based heterogeneous catalyst. *Clean. Eng. Technol.* **2022**, *8*, 100501. [[CrossRef](#)]
42. Patil, P.D.; Deng, S. Optimization of biodiesel production from edible and non-edible vegetable oils. *Fuel* **2009**, *88*, 1302–1306. [[CrossRef](#)]
43. Marques Correia, L.; Cecilia, J.A.; Rodríguez-Castellón, E.; Cavalcante, C.L.; Vieira, R.S. Relevance of the physicochemical properties of calcined quail eggshell (CaO) as a catalyst for biodiesel production. *J. Chem.* **2017**, *2017*, 5679512. [[CrossRef](#)]
44. Kirubakaran, M. Eggshell as heterogeneous catalyst for synthesis of biodiesel from high free fatty acid chicken fat and its working characteristics on a CI engine. *J. Environ. Chem. Eng.* **2018**, *6*, 4490–4503.
45. Pirani, S.; Hashaikeh, R. Nanocrystalline cellulose extraction process and utilization of the byproduct for biofuels production. *Carbohydr. Polym.* **2013**, *93*, 357–363. [[CrossRef](#)]
46. Habibi, Y.; Lucia, L.A.; Rojas, O.J. Cellulose nanocrystals: Chemistry, self-assembly, and applications. *Chem. Rev.* **2010**, *110*, 3479–3500. [[CrossRef](#)]
47. Siqueira, G.; Bras, J.; Dufresne, A. *Luffa cylindrica* as a lignocellulosic source of fiber, microfibrillated cellulose, and cellulose nanocrystals. *BioResources* **2010**, *5*, 727–740. [[CrossRef](#)]
48. Iranmahboob, J.; Nadim, F.; Monemi, S. Optimizing acid-hydrolysis: A critical step for production of ethanol from mixed wood chips. *Biomass Bioenergy* **2002**, *22*, 401–404. [[CrossRef](#)]
49. Duran, N.; Lemes, A.P.; Duran, M.; Freer, J.; Baeza, J. A minireview of cellulose nanocrystals and its potential integration as co-product in bioethanol production. *J. Chil. Chem. Soc.* **2011**, *56*, 672–677. [[CrossRef](#)]
50. Khine, E.E.; Koncz-Horvath, D.; Kristaly, F.; Ferenczi, T.; Karacs, G.; Baumli, P.; Kaptay, G. Synthesis and characterization of calcium oxide nanoparticles for CO<sub>2</sub> capture. *J. Nanopart. Res.* **2022**, *24*, 139. [[CrossRef](#)]

51. Varona, E.; Tres, A.; Rafecas, M.; Vichi, S.; Barroeta, A.C.; Guardiola, F. Methods to determine the quality of acid oils and fatty acid distillates used in animal feeding. *MethodsX* **2021**, *8*, 101334. [[CrossRef](#)]
52. Chai, M.; Tu, Q.; Lu, M.; Yang, Y.J. Esterification pretreatment of free fatty acid in biodiesel production, from laboratory to industry. *Fuel Process. Technol.* **2014**, *125*, 106–113. [[CrossRef](#)]

**Disclaimer/Publisher's Note:** The statements, opinions and data contained in all publications are solely those of the individual author(s) and contributor(s) and not of MDPI and/or the editor(s). MDPI and/or the editor(s) disclaim responsibility for any injury to people or property resulting from any ideas, methods, instructions or products referred to in the content.